Nuclear Spin-Lattice Relaxation in Alkali Halides at Low Temperatures*

C. E. TARR,† L. M. STACEY, AND C. V. BRISCOE
The University of North Carolina, Chapel Hill, North Carolina
(Received 25 August 1966)

The spin-lattice relaxation time T_1 has been measured for the Br^{79} and Br^{81} species in NaBr and LiBr and for the I^{127} species in NaI and RbI in the temperature range 15–77.3°K and also at room temperature, using the 180°-90° pulse technique. The data were fitted to the Van Kranendonk theory using several theoretical phonon spectra. The Van Kranendonk theory satisfactorily accounts for the gross temperature dependence of T_1 over the entire range investigated. A consistent deviation of T_1 to larger values than those predicted by the theory was noted in all of the samples in the range $\simeq$ 30–60°K. The theory is unable to account for these deviations in detail, but the results indicate that optical-phonon relaxation is important even at these low temperatures.

INTRODUCTION

FOR nonmetallic solids, the spin-lattice relaxation time of nuclei with electric quadrupole moments is much shorter than that predicted for magnetic dipole-dipole relaxation. This is due to coupling of the electric quadrupole moment to the lattice by means of fluctuating electric field gradients present at the nuclear sites. This quadrupolar spin-lattice relaxation mechanism is provided by a Raman process in which the energy of a nuclear spin transition is absorbed by the lattice with the emission of one phonon and the absorption of a second. The energy difference of the two phonons is the Larmor energy. Such a two-phonon process is highly favored over a direct process, since, in a direct process, only those phonons with the Larmor energy can participate, while, for a two-phonon process, the only constraint is on the phonon energy difference.

A suitable theory of quadrupolar relaxation was proposed by Van Kranendonk[1] which will be discussed in more detail below. In this theory the transition probabilities are summed over the phonon states with the proper energy difference. Thus the resulting average transition probability contains an expression integrated over the phonon density of states. This transition probability and the associated spin-lattice relaxation time T_1 should, therefore, be somewhat sensitive, although perhaps not markedly so, to the more prominent details of the phonon spectrum.

The present work was undertaken to determine what information about the phonon spectrum could be obtained from an accurate knowledge of the temperature dependence of T_1. This temperature dependence was investigated in the range 15–77.3°K, since this is the region of greatest change of T_1 with temperature and because of the greater accuracy possible due to the larger signals encountered. Also, this temperature range was chosen to provide a more extensive test of the applicability of the Van Kranendonk theory to these crystals, as most previous work was done at somewhat higher temperatures. At these higher temperatures, the Van Kranendonk theory predicts a $T_1 \propto 1/T^2$ which is a satisfactory description of the experiments in that region. Low-temperature data are needed, however, to provide a more complete test of the theory.

Alkali halide single crystals were chosen because of the considerable quantity of relevant data, both experimental and theoretical, available. Measurements were made only on the halide nuclei, as these yield somewhat more tractable T_1's than those of the alkali nuclei which are several orders of magnitude longer.

All of the specimens examined have the NaCl (fcc) structure, and it would appear at first that the electric field gradient should vanish because of symmetry. This is not the case in a real crystal, however, since impurities and strains destroy the local symmetries sufficiently to produce net static electric field gradients. Fortunately, T_1 is independent of strain and impurity concentration over a wide range of such content, except at very low temperatures ($\lesssim$10°K) where impurity relaxation becomes dominant. Several measurements were made at 77.3°K and at room temperature on a Tl-doped NaI scintillating crystal. The results indicated considerable broadening of the resonance line, but T_1 agreed within the experimental uncertainty with the data obtained on optically pure NaI. Briscoe and Squire[2] reported a study of single-crystal and powder data on KI which indicates that T_1 is the same for both specimens within their experimental uncertainty, except at the lowest temperatures, where impurity relaxation is becoming dominant. There is good evidence that impurity relaxation was much stronger in the powder sample than in the single crystal. This may have been due to absorbed water in the powder sample. Finally, recent work in metals shows no measurable effect of strains on T_1.[3]

* This work was supported by the U. S. Air Force Office of Scientific Research under Grant No. AF-AFOSR-645-64 and by the Advanced Research Projects Agency under Contract No. SD-100.

† Present address: University of Pittsburgh, Pittsburgh, Pennsylvania.

[1] J. Van Kranendonk, Physica **20**, 781 (1954).

[2] C. V. Briscoe and C. F. Squire, Phys. Rev. **112**, 1540 (1958).

[3] D. Cutler (private communication).

EXPERIMENTAL PROCEDURE

A conventional pulse apparatus was constructed for these experiments. This apparatus was programmed by pulse-timing circuitry similar in design to that reported by Schwartz,[4] and was capable of supplying a variety of accurately timed pulse sequences.

The timing circuitry was used to trigger commercial pulse-width control units, which in turn determined the duration of a main gate pulse.

This main gate generator was used to gate a 10-MHz crystal-controlled oscillator-gated amplifier similar to the Blume circuit.[5] The oscillator-gated amplifier provided grid drive for a 6252/AX9910 operating in class C as a tuned, push-pull amplifier. This rf power amplifier was coupled through a swinging link and a matching network into the sample coil. The sample coil probe was matched into a LEL i.f. amplifier, factory modified for fast recovery. Additional receiver-transmitter isolation was attained by inserting crossed diodes between the rf power amplifier and the matching network.

The single coil probe was used because of the severe size restrictions imposed by the magnet gap and Dewar dimensions. Although the single coil design had the obvious disadvantage of producing a higher level of receiver saturation than a crossed coil, the recovery time of the system which was limited by ringing in the sample coil was still an acceptable 15 μsec.

The transmitter described above produced rf magnetic fields of $\simeq$40 G, which corresponds to a 90° pulse length of $\simeq$8 μsec for the I^{127} resonance in NaI.

The samples were obtained from Semi-Elements, Inc., Saxonburg Boulevard, Saxonburg, Pennsylvania. All of the samples were cylindrical, optically pure single crystals and were $\frac{1}{2}$ in. in diameter and approximately $\frac{5}{8}$ in. in length. The [110] axis was aligned along the cylindrical axis of the crystal, and was thus perpendicular to the magnetic field direction.

The sample coil was suspended in a double glass Dewar system on a stainless steel coaxial cable that was separated with Teflon spacers and terminated by a vacuum tight BNC connector. This assembly had a capacitance of $\simeq$30 pF, which was sufficiently small to allow placement of the variable resonating capacitance outside the Dewar without unduly sacrificing the Q of the circuit.

Temperatures in the ranges 15–20.4°K and 63–77.3°K were obtained by varying the vapor pressure of liquid hydrogen and nitrogen, respectively. In these ranges, the temperature was determined to about 0.05°K using a mercury manometer. The temperature stability in these ranges was better than 0.2°K for periods of several hours.

A gas refrigerator was used to produce temperatures in the range 20–60°K. The gas refrigerator consisted of a vacuum-jacketed transfer line leading from a storage Dewar of liquid helium to the interior of the sample Dewar and was terminated in the vicinity of the sample coil. The storage Dewar of liquid helium was maintained at an over pressure of several oz/in.^{2} by a ballast tank to ensure a uniform transfer rate. The pressure inside the sample Dewar was reduced by pumping through a precision needle valve. The liquid helium vaporized in the transfer line, and the resulting cold gas was forced past the sample coil by the pressure difference in the sample and storage Dewars. A heat sink was mounted on the end of the helium transfer tube slightly above the sample to ensure temperature stability. Styrofoam baffles were used in the sample Dewar to increase turbulence in the gas flow. This increase in gas-flow impedance was quite effective in maintaining a uniform temperature gradient in the Dewar.

The temperature in the gas refrigerator was measured with a copper-constantan thermocouple referenced to 0°C, and small fluctuations in temperature were monitored with a platinum resistance thermometer.

Using the gas system, the sample temperature could be measured with an estimated absolute accuracy of better than 2°K in the range 20–60°K. Temperatures in this region could be maintained within 0.5°K for periods of several hours.

To compensate for aging and strain in the thermocouple, the nitrogen ice-point emf was measured after every run, and the unknown ice-point emf's were corrected accordingly against published copper-constantan calibration standards.

All of the data were taken at 10 MHz, using a 180°-90° pulse sequence. This method is somewhat more tedious than a saturation 90°-90° pulse sequence for long relaxation times, but, if the data are properly treated, yields a higher degree of accuracy.

The two chief factors that limit the accuracy of the 180°-90° pulse method are the nonlinearity of the receiver response for small signals and imperfections in the 180° pulse.

The nonlinearity of the receiver response gives rise to a disparity in the values of T_1 obtained from a consideration of only the negative (pre-null) or only the positive (post-null) magnetization at a time τ following the 180° pulse.

A linear extrapolation of the receiver response curve intersects the output axis at a negative value. Since this output voltage is to be a measure of the magnetization, a constant voltage had to be added to all of the measured voltages above the nonlinear region to make them proportional to the magnetization. The signals in the nonlinear region were ignored, as it is difficult to correct them properly. This does not represent a significant loss of information, however, as the nonlinear signal amplitude is only about 5% of the average signal amplitude. As this effect is principally due to the nonlinearity of the detection diode at low

[4] J. Schwartz, Rev. Sci. Instr. **28**, 780 (1957).
[5] R. J. Blume, Rev. Sci. Instr. **32**, 554 (1961).

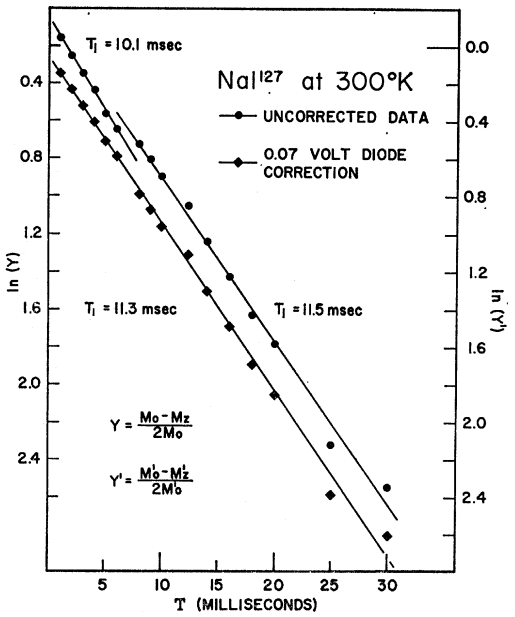

FIG. 1. Effect of the diode correction on the raw data. The upper two curves show the raw data M_0 and M_z fit to single exponential decay. The lower curve shows the data $M_0' = M_0 + C$ and $|M_z'| = |M_z| + C$ fit to single exponential decay using a diode correction C.

signal levels, the additive correction will be referred to as a "diode correction."

Suppose that the relaxation has a single exponential time constant T_1 and that the data have been suitably corrected for nonlinearity in the receiver response. If M_0 is the equilibrium magnetization and M_z is the magnetization at a time τ following a 180° pulse, then, if the data are plotted on a semilogarithmic scale of $(M_0 - M_z)/2M_0$ versus τ, imperfections in the 180° pulse give rise to a straight line that falls below the origin at $\tau = 0$. This is due to a slight difference in the initial condition from the ideal $M_z(0) = -M_0$.

As all of the specimens investigated exhibited single exponential relaxation, both the diode correction and the imperfections in the 180° pulse are easily taken into account by fitting the data to an expression of the form

$$A + B\tau = \ln \frac{M_0' - M_z'}{2M_0'}, \qquad (1)$$

where A is a measure of the deviation from a 180° pulse. In Eq. (1) $M_0' = M_0 + C$ and $|M_z'| = |M_z| + C$, where M_0 and M_z are uncorrected values of the magnetization and C is the diode correction. The constant A is the miss at the origin of a plot of the right side of Eq. (1) against τ. The effect of the diode correction on the pre-null data is to decrease its slope, i.e., to increase the value of T_1 determined by this data, and to reduce the miss at the origin. The effect of the diode correction on the post-null data, on the other hand, is very slight, changing only the intercept. The over-all effect of the diode correction is to bring the slopes of the two segments of the data into a single slope that is nearly equal to that of the uncorrected post-null data. The effect of the diode correction is illustrated in Fig. 1.

The error in the 180° pulse discussed above makes the often used null-point method less accurate for specimens with broad resonance absorption lines than the method used here. Also, the accuracy of the null-point method is impaired by the fact that owing to the nonlinear operation of the receiver for small signals, the null point is not sharp, but is a rather broad minimum.

Least-squares analyses of the data, fit to Eq. (1), were made. For these fits the data were used in four segments: pre-null, post-null, all data excepting the null point, and all of the data including the null point. These fits were made for the raw data, that is, for zero diode correction, and again using the proper diode correction.

The diode correction was determined experimentally by examining the rms error in the fit of all of the data excepting the null point over a large range of values of the diode correction. The rms error was found to be a rather sharply notched function of the diode correction and to reach a minimum for a small diode correction ($\simeq$0.07 V) that was in excellent agreement with the value obtained from a linear extrapolation of the receiver response curve.

The scatter of the individual data points about the least-squares-fitted lines was 2–5%. This 2–5% scatter represents the random scatter in the experiments due to such things as jitter in the pulse lengths, inaccuracies in reading the voltages on the oscilloscope face, etc. Since there were sources of systematic error present in the experiment, notably in temperature measurement using the gas refrigerator, the total experimental uncertainty is somewhat higher than that reflected in the scatter of the data. An uncertainty of $\pm 10\%$ is claimed for all of the measurements, which is a somewhat generous overestimate over most of the temperature range investigated.

THEORY

Van Kranendonk[1] has developed a perturbation calculation of the transition probabilities for quadrupolar relaxation, considering an isotropic distribution of phonon frequencies and polarization and considering interactions due to nearest neighbors only.

The transition probability between nuclear spin states m and $m+\mu$ for lattice transitions λ to λ' under a quadrupole perturbation Hamiltonian H_Q is given by

$$P(m, m+\mu) \propto \int_0^{\omega_m} k^4 f(\omega_k)^2 \sum \{H_Q(\lambda,\lambda')^2\} d\omega_k, \qquad (2)$$

where $f(\omega)$ is related to the phonon density of states by $f(\omega) \propto \rho(\omega)/k^2$.

For a Debye phonon distribution, Eq. (2) may be reduced to a form

$$P(m, m+\mu) \propto \gamma^2 |Q_{\mu m}|^2 T^{*2} \sum_{n=1}^{4} N_{\mu n} D_n(T^*), \quad (3)$$

where $Q_{\mu m}$ are quadrupole matrix elements between nuclear spin states, T^* is the reduced temperature T/θ_D, and the D_n are given by

$$D_n(T^*) = T^* \int_0^{1/T^*} \frac{x^2 e^x}{(e^x-1)^2} L_n(cT^*x)dx. \quad (4)$$

In Eq. (4), the L_n are geometric functions arising from averaging over phonon states, etc., implied by the initial assumptions. The factor γ in Eq. (3) includes both the strength of the quadrupole interaction and the antishielding parameter,[6,7] which are the same for all nuclear species in a given crystal at a given temperature.

If an Einstein δ-function distribution is used in place of the Debye distribution above, T_1 is given by

$$T_1 \propto \gamma^2 |Q_{\mu m}|^2 \sinh^2(\theta_E/2T). \quad (5)$$

Numerical integrations of the functions D_n in Eqs. (3) and (4) were performed over a wide range of values of T^* to provide accurate interpolations of Van Kranendonk's results. These computed values were used to fit the temperature dependence observed in the present work.

Several other contributions to the theory of quadrupole relaxation should be mentioned for completeness. Yosida and Moriya[8] have treated the effects of covalency on T_1, and Kondo and Yamashita[9] have done somewhat more complicated calculations that include overlap of the ionic wave functions.

It is important to note that covalent corrections do not predict a temperature dependence of T_1 that is different from that of the Van Kranendonk theory, aside from effects due to the temperature dependence of the chemical shift. Such temperature dependence of the chemical shift can be seen, cf. Konda,[10] to be entirely negligible. The covalent corrections, then, provide an improvement in the magnitude of T_1, but do not predict a different temperature dependence from that of the Van Kranendonk theory.

Wikner, Blumberg, and Hahn[11] considered the effects of the electric dipole moment induced by the optical phonons. This electric dipole moment can interact strongly with the electric quadrupole moment by means of the large electric field gradients produced at the nucleus.

[6] R. M. Sternheimer and H. M. Foley, Phys. Rev. **92**, 1460 (1953).
[7] H. M. Foley, R. M. Sternheimer, and D. Tycko, Phys. Rev. **93**, 734 (1954).
[8] K. Yosida and T. Moriya, J. Phys. Soc. Japan **11**, 33 (1956).
[9] J. Kondo and J. Yamashita, J. Chem. Phys. Solids **10**, 245 (1959).
[10] T. Konda, J. Phys. Soc. Japan **10**, 85 (1955).
[11] E. G. Wikner, W. E. Blumberg, and E. L. Hahn, Phys. Rev. **118**, 631 (1960).

TABLE I. Comparison of room-temperature data with those of previous work.

Crystal	Nucleus	T_1 (seconds) WBH[a]	Weber[b]	This work
NaI	I^{127}	0.012	0.012	0.011
NaBr	Br^{79}	0.050	···	0.047
	Br^{81}	0.071	···	0.072

[a] E. G. Wikner, W. E. Blumberg, and E. L. Hahn, Phys. Rev. **118**, 631 (1960).
[b] M. J. Weber, Phys. Rev. **130**, 1 (1963).

Following their notation, the Wikner, Blumberg, and Hahn theory predicts a relaxation time given by

$$\frac{1}{T_1} = \left\{1 + A\left(\frac{d\mu}{d\epsilon}\right)^2\right\} \frac{1}{T_1(\text{acoustic})}, \quad (6)$$

where T_1(acoustic) is the value of T_1 obtained from the Van Kranendonk theory, A is a constant characteristic of the crystal and the nuclear spin, μ is the electric dipole moment, and ϵ is the ionic displacement.

This theory provides a relatively simple means of explicitly incorporating the optical phonons, but it predicts only a very slight change in the temperature dependence from the Van Kranendonk theory at temperatures below which the optical modes are significantly populated.

Finally, Joshi, Gupta, and Das[12] have combined the Van Kranendonk theory with that of Wikner, Blumberg, and Hahn. They have used the Van Kranendonk theory to account for acoustic relaxation processes for a general calculated phonon spectrum, cf. Karo[13,14] and Karo and Hardy,[15] and they have used the dipolar theory of Wikner, Blumberg, and Hahn to account specifically for the optical phonon relaxation mechanisms.

The temperature dependence of T_1 predicted by this hybrid theory provides rather good agreement with experiment in the middle to high temperature range ($\simeq$70–300°K), but predicts too slow a variation in T_1 at lower temperatures. An approach of this type, however, could be quite fruitful, if a more realistic inclusion of the phonon dispersion relations could be made.

EXPERIMENTAL RESULTS AND DISCUSSION

Room-temperature measurements were made for comparison to previous work as a check on the apparatus and experimental technique. This comparison is shown in Table I below.

No other data were available for RbI, and no data for LiBr, which has been measured by Weber,[16] are

[12] S. K. Joshi, K. D. Gupta, and T. P. Das, Phys. Rev. **134**, A693 (1964).
[13] A. M. Karo, J. Chem. Phys. **31**, 1489 (1959).
[14] A. M. Karo, J. Chem. Phys. **33**, 7 (1960).
[15] A. M. Karo and J. R. Hardy, Phys. Rev. **129**, 2024 (1963).
[16] M. J. Weber, Phys. Rev. **130**, 1 (1963).

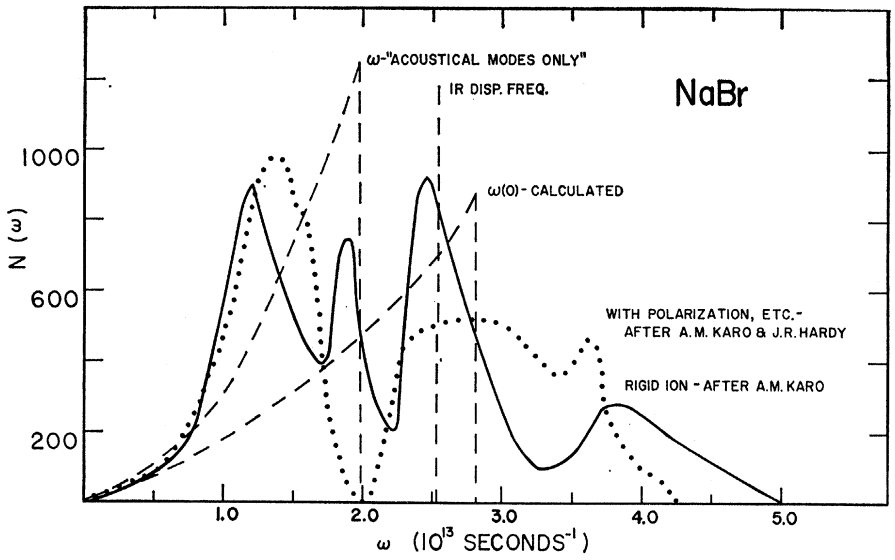

FIG. 2. Typical theoretical phonon distributions used as guides in fitting the data to the Van Kranendonk theory. The solid line shows the results of a rigid-ion calculation by Hardy (Ref. 13) and the dotted line shows the results of a refined calculation by Karo and Hardy (Ref. 15) that includes effects due to ionic polarization, etc. The left-hand dashed line is a Debye spectrum cut off to include only the acoustic phonons. The right-hand dashed line is a Debye spectrum using Hardy's calculated 0°K Debye temperature. The vertical dashed line indiates an Einstein δ-function peak at the Reststrahl frequency.

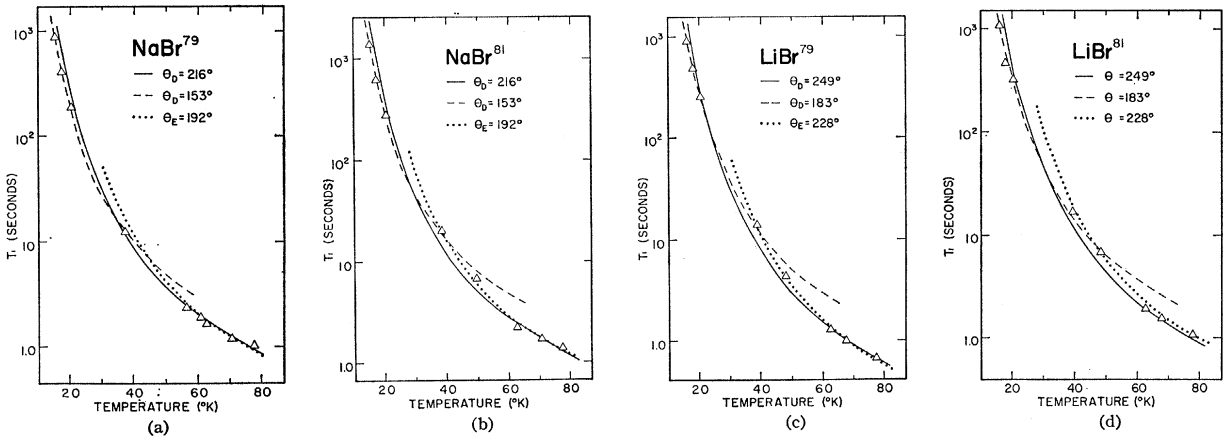

FIG. 3. The Van Kranendonk theory fitted to the experimental results for the Br^{79} and Br^{81} species in NaBr and LiBr. The solid curves are fits using calculated 0°K Debye distributions, the dashed curves are fits using Debye distributions cut off to include only the acoustic phonons, and the dotted curves are fits using Einstein peaks at the Reststrahl frequencies. All of the curves are normalized for best fit.

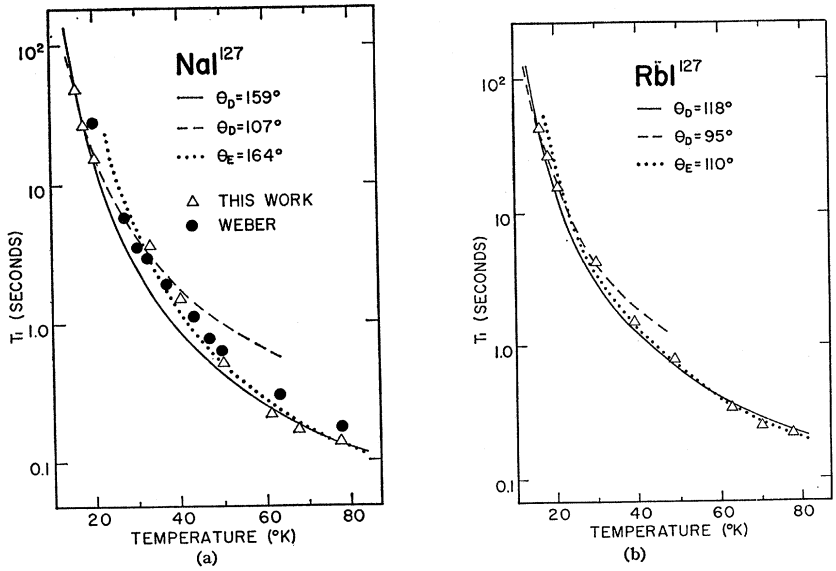

FIG. 4. The Van Kranendonk theory fitted to the experimental results for the I^{127} resonances in NaI and RbI. The solid curves are fits using calculated 0°K Debye distributions, the dashed curves are fits using Debye distributions cut off to include only the acoustic phonons, and the dotted curves are fits using Einstein peaks at the reststrahl frequencies. All of the curves are normalized for best fit. Figure 4(a) includes data by Weber (Ref. 16).

shown for reasons given in the presentation of the data below. As the primary emphasis of the present work is on the temperature range 15–80°K, the discussion of the room-temperature data will be postponed until the end of this section.

Comparison with Theory

Figure 2 shows typical theoretical phonon spectra used as a guide in fitting the T_1 data to theoretical calculations. The solid line is a rigid-ion calculation by Karo,[13] and the dotted line is a calculation by Karo and Hardy[15] that includes the effect of ionic polarization, etc. for NaBr.

The experimental temperature dependence of T_1 in the range 15–80°K for the nuclei investigated in this work is shown in Figs. 3 and 4. The solid lines in these figures are theoretical curves calculated from the Van Kranendonk theory with Debye temperatures calculated at 0°K by Karo. These calculated 0°K Debye temperatures are not in very close agreement with the available specific-heat data, as can be seen from Karo's work, but they do, however, serve as a good average of the Debye temperature in the 0–300°K range. Choosing the characteristic temperature in this manner provides a systematic means of fitting the data in the absence of sufficient experimental specific-heat data. The 0°K Debye distribution is shown as the right-hand dashed line in Fig. 2.

The dashed lines in Figs. 3 and 4 are theoretical curves calculated from the Van Kranendonk theory with Debye distributions cut off so as to include only the acoustic phonons. These characteristic temperatures are good averages of the Debye temperatures at very low temperatures and are more in the spirit of the Van Kranendonk calculations than the previous fits, as the Van Kranendonk theory explicitly accounts only for the acoustic modes.

The dotted lines in Figs. 3 and 4 show the Van Kranendonk theory fit to the data using an Einstein δ-function peak at the reststrahl frequency. The fits in these regions are quite good and are some indication that the optical phonons are important to the quadrupole relaxation even at relatively low temperatures.

The solid lines in Figs. 3 and 4 are normalized for best fit over the entire low-temperature range (15–80°K). The dashed and dotted lines are normalized for best fit in the lower ($\simeq$15–40°K) and higher ($\simeq$40–80°K) regions, respectively.

Sodium Bromide and Lithium Bromide

The alkali bromides provide especially useful tests of the theory, as Br^{79} and Br^{81} are isotopes of nearly equal natural abundance. Comparison of the relaxation times of the two bromine isotopes enables a comparison of two different nuclear species in very nearly identical environments.

Since the transition probability [Eq. (3)] is proportional to the square of the electric quadrupole moment, the ratio of the relaxation times of the two nuclear species in a given sample should be inversely proportional to the ratio of the squares of the corresponding quadrupole moments, if the relaxation process is due to the quadrupole interaction.

Examination of this ratio for NaBr indicates that the relaxation mechanism is quadrupolar over the entire temperature range investigated. This ratio for the LiBr data shows no departure, within experimental uncertainty, from quadrupole relaxation for temperatures in the range 45–80°K. There is, however, a consistent departure to lower values of the ratio T_1^{81}/T_1^{79} in LiBr below $\simeq$45°K. This departure, though consistent, is only slightly outside the experimental uncertainty. This effect may be attributable to slightly different temperature dependences of the quadrupolar coupling constant, the Sternheimer antishielding parameter, or both. Also, the bromine resonances in LiBr are more broadened than those in NaBr, so that some difficulty may have arisen from an inadequate coverage of the resonance lines in LiBr.

The data for the Br^{79} and Br^{81} nuclei in NaBr are shown in Figs. 3(a) and 3(b), and those for LiBr are shown in Figs. 3(c) and 3(d). The fits to the data using the calculated 0°K Debye distributions in the Van Kranendonk theory satisfactorily account for the gross temperature dependence over the entire range of temperatures investigated. There are noticeable departures from these curves for each of these nuclei in the range 40–60°K. This is due to structure in the phonon spectra that is not accounted for satisfactorily in the Debye approximation. This departure should be larger for larger mass ratios, as the structure in the phonon spectra becomes more sharply peaked and the peak separation greater with increasing ionic mass ratio. This supposition is supported by the appearance of a larger departure in the LiBr data, with a halide/alkali ionic mass ratio $\simeq$11.5, than in the NaBr data, with a mass ratio $\simeq$3.5.

The fits to the lower ($\simeq$15–45°K) and higher ($\simeq$45–80°K) temperature regions of the low-temperature data are quite good. The fits at the lower temperatures indicate that the Van Kranendonk theory provides a good description of the relaxation process in the region where the optical modes are virtually unpopulated, as was to be expected. The fits to the higher temperature data, using Einstein peaks at the Reststrahl frequencies, indicate the importance of the optical phonons even at relatively low temperatures.

Sodium Iodide and Rubidium Iodide

The results of the measurements on I^{127} in NaI and RbI are shown in Figs. 4(a) and 4(b), respectively.

Again, in these samples the calculated 0°K Debye distributions in the Van Kranendonk theory satis-

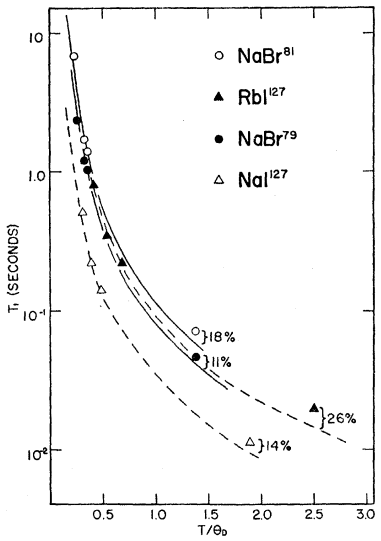

Fig. 5. Relation of room-temperature measurements on NaBr, NaI, and RbI to the low-temperature data. The curves shown are extensions of the solid curves (Van Kranendonk theory using calculated 0°K Debye distributions) in Figs. 3 and 4. The deviations of the theoretical curves from the room-temperature points are shown in percent.

factorily account for the gross temperature dependence of T_1 over the entire temperature range investigated. Also the fits to the lower and higher ends of the low-temperature data support the assumptions made above.

The relatively small departure of the data from the 0°K fit found for RbI is expected because of the small ionic mass ratio of $\simeq$1.5. This mass argument is not clearly applicable to this case, however, as the transverse optical and longitudinal acoustic branches are almost coincident in RbI. This is reflected in the closeness of the characteristic temperatures corresponding to the acoustic phonons and the reststrahl frequency.

The departure from the theoretical curve for NaI, on the other hand, is relatively large (ionic mass ratio $\simeq$4.7) and is in good agreement with the data of Weber,[16] some of which is shown in Fig. 4(a).

Room-Temperature Data

Figure 5 shows the room-temperature data in relation to the low-temperature data. The curves in Fig. 5 are extensions of the solid curves shown in the fits to the low-temperature data. The room-temperature points all lie above the theoretical curves, indicating the importance of the optical mode relaxation at higher temperatures. The Van Kranendonk theory does not explicitly account for the optical modes, and hence predicts too rapid a decrease of T_1 at higher temperatures. This is due primarily to the fact that there are fewer modes populated near room temperature in the actual phonon distribution than is predicted by a Debye distribution, as can be seen in Fig. 2. No room-temperature data are shown for LiBr, as the primary relaxation mechanism in this range is vacancy diffusion.[16]

CONCLUSIONS

The over-all fit of the Van Kranendonk theory using a calculated 0°K Debye temperature agrees sufficiently well with the data over the entire temperature range to conclusively show that the primary contribution to the relaxation is properly accounted for by this relatively simple theory. The consistent deviations for temperatures in the range $\simeq$30–60°K for all of the samples can be accounted for by the structure in the phonon spectra. The Debye temperature is strongly temperature-dependent in this region and goes through a minimum near this region for all of the specimens. The calculated 0°K Debye temperature represents an average over a large temperature range, so that it is not surprising that the theoretical fits using these average Debye temperatures account for the gross temperature dependence of the data.

The excellent fits to the data at very low temperatures using a Debye spectrum containing only the acoustic modes are also quite plausible in view of the structure of the phonon spectra. At very low temperatures the only modes that are substantially populated, and hence the only modes contributing significantly to the relaxation process, are the acoustic modes. This is the sort of distribution that the Van Kranendonk theory was tailored for, so that it is not surprising that these low-temperature fits are quite good.

The results of the present work, then, show that the principal features of the temperature dependence of T_1 are reasonably well described by the rigid-ion theory of Van Kranendonk. The nature of the theoretical fits to the data indicates that this temperature dependence is somewhat sensitive to the larger details of the phonon spectra, and that data of this kind might be used in conjunction with a suitably improved theory to obtain additional information about these phonon spectra. The results of the various extensions of the theory, such as the work of Joshi, Gupta, and Das,[12] indicate the need for a proper accounting, not only for the structure of the phonon spectra, but also for the dispersion relations involved. Such calculations would be tedious, but it seems that they would be rewarding in light of the experimental results.

ACKNOWLEDGMENTS

It is a pleasure to acknowledge the helpful advice of Professor W. A. Bowers, Professor P. S. Hubbard, and Professor H. Kessemeier of the University of North Carolina Physics Department. We are grateful to W. C. Overton, Jr. of the Los Alamos Scientific Laboratory for an illuminating discussion concerning the proper use of the Debye temperature approximation.